PERGAMON

International Journal of Solids and Structures 39 (2002) 897–910

INTERNATIONAL JOURNAL OF SOLIDS and STRUCTURES

www.elsevier.com/locate/ijsolstr

A realistic estimation of the effective breadth of ribbed plates

John T. Katsikadelis, Evangelos J. Sapountzakis *

Department of Civil Engineering, Institute of Structural Analysis, National Technical University of Athens, Zografou Campus, GR-157 73 Athens, Greece

Received 5 April 2001; in revised form 10 October 2001

Abstract

In this paper a realistic estimation of the effective breadth of a stiffened plate is presented. For the estimation of the effective breadth the adopted model contrary to the models used previously takes into account the resulting inplane forces and deformations of the plate as well as the axial forces and deformations of the beam, due to combined response of the system. The analysis consists in isolating the beams from the plate by sections parallel to the lower outer surface of the plate. The forces at the interface, which produce lateral deflection and inplane deformation to the plate and lateral deflection and axial deformation to the beam, are established using continuity conditions at the interface. The solution of the arising plate and beam problems, which are nonlinearly coupled, is achieved using the analog equation method. After the solution of the plate—beams system is achieved, the distribution of the axial stresses across the plate, resulting from both the bending and the inplane action of the plate, is obtained. Integrating this distribution across the plate the values of the effective breadth are obtained. The influence of these values from the beam stiffness and their variation along the longitudinal direction of the plate are shown as compared with those obtained from various codes through numerical examples with great practical interest.

Keywords: Elastic stiffened plate; Effective breadth; Reinforced plate with beams; Bending; Ribbed plate; Analog equation method

1. Introduction

Today stiffened plates are commonly used in the construction of long span slabs, long river or valley bridge decks or floors of aircraft carriers due to the economic and structural advantages of such systems. Stiffened plate structures are efficient, economical, functional and readily constructed of most common materials.

Two design parameters of stiffened plates, namely effective breadth and effective width, are commonly used in structural engineering for thoroughly different engineering purposes (Schade, 1951; Wang and Rammerstorfer, 1996). Both of these parameters are used to describe the effectiveness of a breadth or width of stiffened plate structures in which the axial stress distribution across the plate is not uniform.

* Corresponding author. Tel.: +301-772-1718; fax: +301-772-1720.
E-mail addresses: jkats@central.ntua.gr (J.T. Katsikadelis), cvsapoun@central.ntua.gr (E.J. Sapountzakis).

0020-7683/02/$ - see front matter
PII: S0020-7683(01)00277-3

The design parameter of *effective breadth* is used when we consider a stiffened plate subjected to lateral loading. Due to the aforementioned loading the plate bends out of its original plane, while the distribution of the axial stresses across the plate is not uniform because of the transmission of shear from the stiffener through the plate (shear lag phenomenon). Defining the effective breadth of the slab (Timoshenko and Goodier, 1951) as the breadth which would sustain a force equal to the actual force in the slab, if the longitudinal stress across the breadth was constant and equal to the theoretical stress at the neutral axis of the slab at the beam edge, the designer is enabled to calculate the bending behaviour of the stiffened structure by the use of simple beam theory.

The design parameter of *effective width* is used when we consider a stiffened plate subjected to inplane compressive loading. Due to local buckling of the plate between the stiffeners the axial stresses distribution across the plate is also not uniform. Using the concept of the effective width, in an analogous manner with that of the effective breadth, the designer may estimate the postbuckling strength of a stiffened plate under compression.

In this paper a realistic estimation of the effective breadth of a stiffened plate is presented. Various definitions of the effective breadth have been given from various researchers depending on the intensity of the approximating constant stress (theoretical stress at the beam edge or at the axis of the stiffening beam) and the inclusion or not of the beam width (Schade, 1951; Wang and Rammerstorfer, 1996; Lee, 1962). For the purpose of this paper the definition given in Timoshenko and Goodier (1951) will be adopted, while for comparison reasons all available definitions will be reported.

For the estimation of the effective breadth or the effective width of stiffened plates, approximate methods such as the finite strip method (Wang and Rammerstorfer, 1996), energy methods (Tsutomu, 1982) or the FEM (Tsutomu, 1993) have been employed. In all the aforementioned methods the adopted model for the analysis of the plate–beams system neglects the shear forces at the interfaces and the resulting inplane forces and deformations of the plate as well as the axial forces and deformations of the beam. This assumption results in discrepancies from the actual response of the stiffened plate.

In this paper for the estimation of the effective breadth the adopted model contrary to the models used previously takes into account the resulting inplane forces and deformations of the plate as well as the axial forces and deformations of the beam, due to combined response of the system. The analysis consists in isolating the beams from the plate by sections parallel to the lower outer surface of the plate. The forces at the interface, which produce lateral deflection and inplane deformation to the plate and lateral deflection and axial deformation to the beam, are established using continuity conditions at the interface. The solution of the arising plate and beam problems, which are nonlinearly coupled, is achieved using the analog equation method (AEM) (Sapountzakis and Katsikadelis, 2000). After the solution of the plate–beams system is achieved, the distribution of the axial stresses across the plate, resulting from both the bending and the inplane (arising from the shear forces at the interfaces) action of the plate, is obtained. Integrating this distribution across the plate and following the aforementioned definition of the effective breadth we obtain its values in the longitudinal direction of the plate. The influence of these values from the beam stiffness and their variation along the longitudinal direction of the plate are shown as compared with those obtained from various codes through numerical examples with great practical interest.

2. Statement of the problem

2.1. Modeling of the ribbed plate

Consider a thin elastic plate having constant thickness h_p, occupying the domain Ω of the x, y plane and stiffened by a set of parallel beams. The plate may have J holes while its boundary $\Gamma = \cup_{j=0}^{J} \Gamma_j$ may be piecewise smooth (Fig. 1). For the sake of convenience the x axis is taken parallel to the beams. The plate is

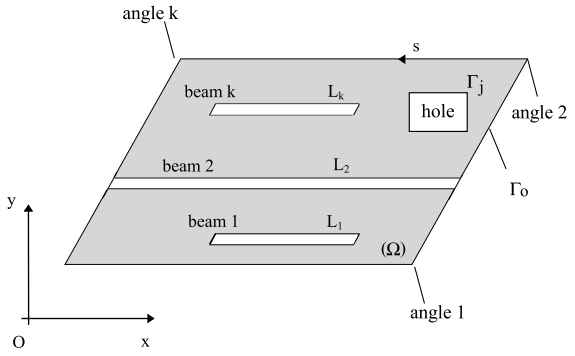

Fig. 1. Two dimensional region Ω occupied by the plate.

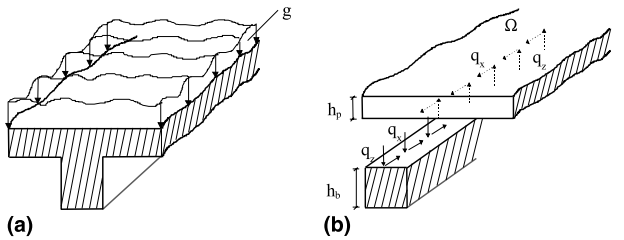

Fig. 2. Thin elastic plate stiffened by beams (a) and isolation of the beams from the plate (b).

subjected to the lateral load $g = g(\boldsymbol{x})$, $\boldsymbol{x} : \{x, y\}$ and is supported on its boundary, whereas the beams may have point supports.

For the solution of the problem at hand and the evaluation of the distribution of the axial stresses across the plate the method presented by Sapountzakis and Katsikadelis (2000) is adopted here. According to this method the stiffening beams are isolated from the plate by sections in the lower outer surface of the plate, while tractions at the fictitious interfaces are taken into account (Fig. 2). These tractions result in the loading of the beam as well as the additional loading of the plate. Their distribution is unknown and is established by imposing displacement continuity conditions at the interfaces.

The integration of the tractions along the width of the beam result in line forces per unit length which are denoted by q_x, q_y and q_z. Taking into account that the torsional stiffness of the beam is small, the traction component q_y, in the direction normal to the beam axis is ignored. The other two components q_x and q_z produce the following loadings along the trace of each beam.

In the plate:

(i) A lateral line load $-q_z$ at the interface.
(ii) A lateral line load $-\partial M_p/\partial x$ due to the eccentricity of the component q_x from the middle surface of the plate. $M_p = q_x h_p/2$ is the bending moment.
(iii) An inplane line body force q_x at the middle surface of the plate.

In each beam:

(i) A transverse load q_z.
(ii) A transverse load $\partial M_b/\partial x$ due to the eccentricity of q_x from the neutral axis of the beam cross section.
(iii) An inplane axial force q_x.

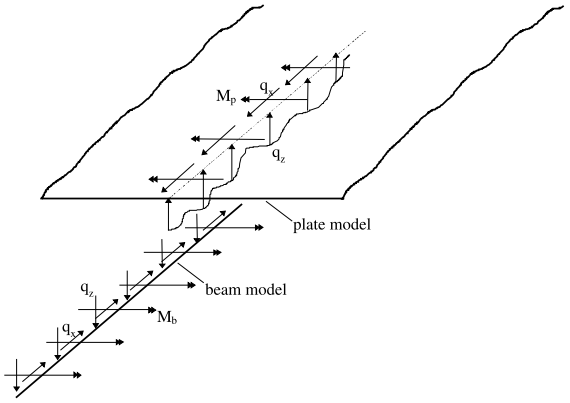

Fig. 3. Structural model of the plate and the beams.

The structural models of the plate and the beams are shown in Fig. 3.

On the base of the above considerations the response of the plate and of the beams may be described by the following boundary value problems.

(i) For the plate: The plate undergoes transverse deflection and inplane deformation. Thus, for the transverse deflection we have

$$D\nabla^4 w_{\mathrm{p}} - \left(N_x \frac{\partial^2 w_{\mathrm{p}}}{\partial x^2} + 2N_{xy} \frac{\partial^2 w_{\mathrm{p}}}{\partial x\, \partial y} + N_y \frac{\partial^2 w}{\partial y^2} \right) = g - \sum_{k=1}^{K} \left(q_z^{(k)} + \frac{\partial M_{\mathrm{p}}^{(k)}}{\partial x} \right) \delta(y - y_k) \quad \text{in } \Omega \tag{1}$$

$$\alpha_1 w_{\mathrm{p}} + \alpha_2 V_{\mathrm{n}} = \alpha_3 \quad \text{on } \Gamma \tag{2a}$$

$$\beta_1 \frac{\partial w_{\mathrm{p}}}{\partial n} + \beta_2 M_{\mathrm{n}} = \beta_3 \tag{2b}$$

where $w_{\mathrm{p}} = w_{\mathrm{p}}(\boldsymbol{x})$ is the transverse deflection of the plate; $D = E_{\mathrm{p}} h_{\mathrm{p}}^3 / 12(1 - v^2)$ is its flexural rigidity with E_{p} being the elastic modulus and v the Poisson ratio; $N_x = N_x(\boldsymbol{x})$, $N_y = N_y(\boldsymbol{x})$, $N_{xy} = N_{xy}(\boldsymbol{x})$ are the membrane forces per unit length of the plate cross section; $\delta(y - y_k)$ is the Dirac's delta function in the y direction; M_{n} and V_{n} are the bending moment normal to the boundary and the effective reaction along it, respectively, and they are given as

$$M_{\mathrm{n}} = -D \left(\frac{\partial^2 w_{\mathrm{p}}}{\partial n^2} + v \frac{\partial^2 w_{\mathrm{p}}}{\partial t^2} \right) \tag{3}$$

$$V_{\mathrm{n}} = -D \left[\frac{\partial}{\partial n} \nabla^2 w_{\mathrm{p}} - (v - 1) \frac{\partial}{\partial s} \frac{\partial^2 w_{\mathrm{p}}}{\partial n\, \partial t} \right] \tag{4}$$

Finally, a_i, β_i $(i = 1, 2, 3)$ are functions specified on the boundary Γ.

The boundary conditions (2a) and (2b) are the most general linear boundary conditions for the plate problem including also the elastic support. It is apparent that all types of the conventional boundary conditions (clamped, simply supported, free or guided edge) can be derived form these equations by specifying appropriately the functions a_i and β_i (e.g. for a clamped edge it is $a_1 = \beta_1 = 1$, $a_2 = a_3 = \beta_2 = \beta_3 = 0$).

Since linear plate bending theory is considered, the components of the membrane forces N_x, N_y, N_{xy} do not depend on the deflection w_{p}. They are given as

$$N_x = C\left(\frac{\partial u_p}{\partial x} + v\frac{\partial v_p}{\partial y}\right) \tag{5a}$$

$$N_y = C\left(v\frac{\partial u_p}{\partial x} + \frac{\partial v_p}{\partial y}\right) \tag{5b}$$

$$N_{xy} = C\frac{1-v}{2}\left(\frac{\partial u_p}{\partial y} + \frac{\partial v_p}{\partial x}\right) \tag{5c}$$

where $C = E_p/(1-v^2)$; $u_p = u_p(\boldsymbol{x})$ and $v_p = v_p(\boldsymbol{x})$ are the displacement components of the middle surface of the plate and are established by solving the plane stress problem, which is described by the following boundary value problem (Navier's equations of equilibrium)

$$\nabla^2 u_p + \frac{1+v}{1-v}\frac{\partial}{\partial x}\left[\frac{\partial u_p}{\partial x} + \frac{\partial v_p}{\partial y}\right] + \frac{1}{G_p}q_x\delta(y-y_k) = 0 \quad \text{in } \Omega \tag{6a}$$

$$\nabla^2 v_p + \frac{1+v}{1-v}\frac{\partial}{\partial y}\left[\frac{\partial u_p}{\partial x} + \frac{\partial v_p}{\partial y}\right] = 0 \tag{6b}$$

$$\gamma_1 u_n + \gamma_2 N_n = \gamma_3 \quad \text{on } \Gamma \tag{7a}$$

$$\delta_1 u_t + \delta_2 N_t = \delta_3 \tag{7b}$$

in which $G_p = E_p/2(1+v)$ is the shear modulus of the plate; N_n, N_t and u_n, u_t are the boundary membrane forces and displacements in the normal and tangential directions to the boundary, respectively; γ_i, δ_i $(i = 1, 2, 3)$ are functions specified on Γ.

(ii) For each beam: Each beam undergoes transverse deflection and axial deformation. Thus, for the transverse deflection we have

$$E_b I_b\frac{d^4 w_b}{dx^4} - N_b\frac{\partial^2 w_b}{\partial x^2} = q_z - \frac{\partial M_b}{\partial x} \quad \text{in } L_k,\ k = 1, 2, \ldots, K \tag{8}$$

$$a_1 w_b + a_2 V = a_3 \quad \text{at the beam ends } x = 0, l \tag{9a}$$

$$b_1\frac{\partial w_b}{\partial x} + b_2 M = b_3 \tag{9b}$$

where $w_b = w_b(x)$ is the transverse deflection of the beam; $E_b I_b$ is its flexural rigidity; $N_b = N_b(x)$ is the axial force at the neutral axis; V, M are the reaction and the bending moment at the beam ends, respectively and a_i, b_i $(i = 1, 2, 3)$ par are coefficients specified at the boundary of the beam. It is apparent that all types of the conventional boundary conditions (clamped, simply supported, free or guided edge) can be derived from Eqs. (9a) and (9b) by specifying appropriately the coefficients a_i, b_i (e.g. for a simply supported end it is $a_1 = b_2 = 1$, $a_2 = a_3 = b_1 = b_3 = 0$).

Since linear beam bending theory is considered, the axial force of the beam does not depend on the deflection w_b. The axial deformation of the beam is described by solving independently the boundary value problem i.e.

$$E_b A_b\frac{\partial^2 u_b}{\partial x^2} = -q_x \quad \text{in } L_k,\ k = 1, 2, \ldots, K \tag{10}$$

$$c_1 u_b + c_2 N = c_3 \quad \text{at the beam ends } x = 0, l \tag{11}$$

where N is the axial reaction at the beam ends.

Eqs. (1), (6a), (6b), (8), (10) constitute a set of five coupled partial differential equations including seven unknowns, namely w_p, u_p, v_p, w_b, u_b, q_x, q_z. Two additional equations are required, which result from the continuity conditions of the displacements in the direction of the z and x axes at the interfaces between the plate and the beams. These conditions can be expressed as

$$w_p = w_b \tag{12}$$

$$u_p - \frac{h_p}{2}\frac{\partial w_p}{\partial x} = u_b + \frac{h_b}{2}\frac{\partial w_b}{\partial x} \tag{13}$$

It must be noted that the coupling of Eqs. (1), (6a) and (6b), as well as of Eqs. (8) and (10) is nonlinear due to the terms including the unknown membrane and axial forces, respectively.

2.2. Definitions and estimation of the effective breadth

As it is already mentioned the design parameter of *effective breadth* is used when we consider a stiffened plate subjected to lateral loading. Due to the aforementioned loading the plate bends out of its original plane, while the distribution of the axial stresses across the plate is not uniform because of the transmission of shear from the stiffener through the plate (shear lag phenomenon). The effective breadth of the slab is defined as the breadth that would sustain a force equal to the actual force in the slab, if the longitudinal stress across the breadth was constant and equal to the theoretical stress at the neutral axis of the slab at the beam edge or at the axis of the stiffening beam (depending on the definition).

Following this definition, combining Fig. 4(a) with the following relation

$$b_{\text{eff}} = \frac{\int \sigma_x \mathrm{d}y}{\sigma_e} \tag{14}$$

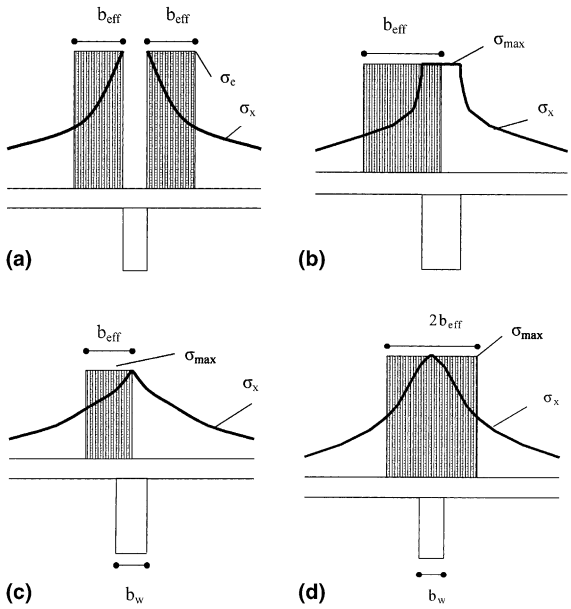

Fig. 4. Effective breadth definitions according (a) to Timoshenko and Goodier (1951), (b) to Schade (1951), (c) to Wang and Rammerstorfer (1996) and (d) to Lee (1962).

the effective breadth can be estimated according to Timoshenko and Goodier (1951). Similarly, concerning other researchers, the values of the effective breadth can be obtained according to Schade (1951) combining Fig. 4(b) with the following relation

$$b_{\text{eff}} = \frac{\int \sigma_x \mathrm{d}y}{\sigma_{\max}} \tag{15}$$

according to Wang and Rammerstorfer (1996) combining Fig. 4(c) with Eq. (15) and according to Lee (1962) combining Fig. 4(d) with the following relation

$$2b_{\text{eff}} = \frac{2\int \sigma_x \mathrm{d}y}{\sigma_{\max}} + b_w \tag{16}$$

In all the aforementioned definitions, the evaluation of the effective breadth presumes the estimation of the distribution of the axial stresses across the plate, which is accomplished as follows.

After the solution of the nonlinear system of equations (1), (6a), (6b), (8), (10), (12) and (13) the unknown plate w_{p} and beam w_{b} deflection, the displacement components u_{p}, v_{p} of the middle surface of the plate, the axial deformation of the beam u_{b} and the interface forces q_x, q_z are established. The axial stresses across the plate result from superposition of the bending and the inplane action of the plate. The axial stresses $(\sigma_x)_{\text{b}}$ due to the bending action of the plate arising from the lateral external loading g, the lateral line load $-q_z$ at the interfaces and the lateral line load $-\partial M_{\text{p}}/\partial x$ due to the eccentricity of the component q_x from the middle surface of the plate are given as

$$(\sigma_x)_{\text{b}} = -\frac{E}{1-\nu^2}\, z\left(\frac{\partial^2 w_{\text{p}}}{\partial x^2} + \nu\frac{\partial^2 w_{\text{p}}}{\partial y^2}\right) \tag{17}$$

The axial stresses $(\sigma_x)_i$ due to the inplane action of the plate arising from the inplane line body force q_x at the middle surface of the plate are given as

$$(\sigma_x)_i = C(u_{\text{p}} + \nu v_{\text{p}}) \tag{18}$$

where $C = E_{\text{p}}/(1-\nu^2)$. Thus, the distribution of the axial stresses across the plate is given as

$$\sigma_x = (\sigma_x)_{\text{b}} + (\sigma_x)_i \tag{19}$$

or using Eqs. (17) and (18)

$$\sigma_x = -\frac{E}{1-\nu^2} z\left(\frac{\partial^2 w_{\text{p}}}{\partial x^2} + \nu\frac{\partial^2 w_{\text{p}}}{\partial y^2}\right) + C(u_{\text{p}} + \nu v_{\text{p}}) \tag{20}$$

Integrating across the plate the evaluated distribution of the axial stresses given from Eq. (20) the effective breadth is estimated according to the aforementioned various definitions. For the purpose of this paper, and having no other particular reason, the definition given in Timoshenko and Goodier (1951) will be adopted (every other definition could also be utilized), while for comparison reasons all available definitions will be used.

3. Numerical solution

The solution of the bending problem of a plate reinforced with beams is accomplished by developing the AEM given in Sapountzakis and Katsikadelis (2000).

According to this method for the plate bending problem we assume w_{p} as the sought solution of the boundary value problem (1), (2a) and (2b). Applying the biharmonic operator to this function we obtain

$$\nabla^4 w_{\text{p}} = q_{\text{p}} \quad \text{in } \Omega \tag{21}$$

Eq. (21) indicates that the solution of the original problem, Eq. (1), can be obtained from the solution of a linear plate bending problem with unit stiffness, under the same boundary conditions and subjected to the fictitious load distribution $q_p(\boldsymbol{x})$. This problem is readily solved if the fictitious loading were known. Thus, the problem is converted to that of establishing the unknown load density $q_p(\boldsymbol{x})$. This is accomplished using BEM as follows.

The solution of Eq. (21) is given in integral form as

$$\varepsilon w_p(\boldsymbol{x}) = \int_\Omega w_p^* q_p \mathrm{d}\Omega - \int_\Gamma \left(w_p^* V_n - \frac{\partial w_p^*}{\partial n} M_n + w_p V_n^* - \frac{\partial w_p}{\partial n} M_n^* \right) \mathrm{d}s \tag{22}$$

where $\varepsilon = 1$, $1/2$ or 0 depending on whether the point $\boldsymbol{x}$ is inside the domain Ω, on the boundary Γ, or outside Ω, respectively and w_p^* is the fundamental solution given as

$$w_p^* = \frac{1}{8\pi} r^2 \ln r \tag{23}$$

The quantities M_n^* and V_n^* are obtained from Eqs. (3) and (4), respectively, by replacing w_p with w_p^*.

Using the integral representation (22) of w_p and its normal derivative for $\boldsymbol{x} \in \Gamma$ together with the boundary conditions (2a) and (2b) the boundary quantities w_p, $\partial w_p/\partial n$, M_n, V_n can be eliminated from the discretized counterpart of Eq. (22) which after collocation at the M domain nodal points and differentiation with respect to x and y yields

$$\{w_p\} = [P]\{q_p\} \tag{24}$$

$$\{w_{p,x}\} = [P_x]\{q_p\} \tag{25a}$$

$$\{w_{p,xx}\} = [P_{xx}]\{q_p\} \tag{25b}$$

$$\{w_{p,yy}\} = \lfloor P_{yy} \rfloor \{q_p\} \tag{25c}$$

$$\{w_{p,xy}\} = \lfloor P_{xy} \rfloor \{q_p\} \tag{25d}$$

where $[P]$, $[P_x]$, $[P_{xx}]$, $\lfloor P_{yy} \rfloor$, $\lfloor P_{xy} \rfloor$ are known $M \times M$ coefficient matrices.

Finally, applying Eq. (1) to the M nodal points inside Ω we obtain

$$D\{q_p\} - ([N_x][P_{xx}] + 2\lfloor N_{xy} \rfloor \lfloor P_{xy} \rfloor + \lfloor N_y \rfloor \lfloor P_{yy} \rfloor)\{q_p\} = \{g\} - [Z]\{q_z\} - [X]\{q_x\} \tag{26}$$

where $[N_x]$, $\lfloor N_{xy} \rfloor$ and $\lfloor N_y \rfloor$ are unknown diagonal $M \times M$ matrices including the values of the inplane forces; $\{q_z\}$ and $\{q_x\}$ are vectors with L elements; L is the total number of the nodal points at the interfaces; $[Z]$ is a position vector which converts the vector $\{q_z\}$ into a vector with length M. The matrix $[X]$ results after approximating the derivative of M_p with finite differences. Its dimensions are also $M \times L$.

For the plane stress problem following the procedure of the AEM presented in Katsikadelis and Kandilas (1994) and using the same boundary and domain discretization the membrane forces for homogeneous boundary conditions (7a) and (7b) ($\gamma_3 = \delta_3 = 0$) are expressed as follows

$$\{N_x\} = [F_x]\{q_x\} \tag{27a}$$

$$\{N_{xy}\} = \lfloor F_{xy} \rfloor \{q_x\} \tag{27b}$$

$$\{N_y\} = \lfloor F_y \rfloor \{q_x\} \tag{27c}$$

where $[F_x]$, $\lfloor F_{xy} \rfloor$ and $\lfloor F_y \rfloor$ are known matrices with dimensions $M \times L$.

Similarly with the plate for the beam bending problem we assume w_b as the sought solution of the boundary value problem described by Eqs. (8), (9a) and (9b). Differentiating this function four times yields

$$\frac{d^4 w_b}{dx^4} = q_b \tag{28}$$

The solution of Eq. (28) is given in integral form as (Banerjee and Butterfield, 1981)

$$w_b(x) = \int_0^l w_b^* q_b ds + \left[w_b^* V - \frac{\partial w_b^*}{\partial x} M + w_b V^* - \frac{\partial w_b}{\partial x} M^* \right]_0^l \tag{29}$$

where w_b^* is the fundamental solution given as

$$w_b^* = \tfrac{1}{12} l^3 (2 + |\rho|^3 - 3|\rho|^2) \tag{30}$$

with $\rho = r/l$, $r = \xi - x$, $x \in L_k$, $k = 1, 2, \ldots, K$, ξ at the beam ends $x = 0$, l and the quantities M^* and V^* are given from the following relations

$$M^* = \tfrac{1}{2} l (1 - |\rho|) \tag{31a}$$

$$V^* = -\tfrac{1}{2} \operatorname{sgn} \rho \tag{31b}$$

Using the integral representation (29) of w_b and its second derivative with respect to x for x on the boundary of the beam together with the boundary conditions (9a) and (9b) the boundary quantities w_b, $\partial w_b/\partial n$, M, V can be eliminated from the discretized counterpart of Eq. (29), which after collocation at the L nodal points at the interfaces (for homogeneous boundary conditions (9a) and (9b) $a_3 = b_3 = 0$) yields

$$\{w_b\} = [B]\{q_b\} \tag{32}$$

where $[B]$ is an $L \times L$ matrix.

Differentiating Eq. (29) with respect to x, eliminating the boundary quantities from the discretized counterpart of these equations and collocating at the L nodal points at the interfaces (for homogeneous boundary conditions $a_3 = b_3 = 0$) we obtain

$$\{w_{b,x}\} = [B_x]\{q_b\} \tag{33a}$$

$$\{w_{b,xx}\} = [B_{xx}]\{q_b\} \tag{33b}$$

where $[B_x]$, $[B_{xx}]$ are known $L \times L$ coefficient matrices.

Finally, applying Eq. (8) to the L nodal points at the interfaces we obtain

$$E_b I_b \{q_b\} - [N_b][B_{xx}]\{q_b\} = \{q_z\} - [Q]\{q_x\} \tag{34}$$

where $[N_b]$ is unknown diagonal $L \times L$ matrix including the values of the inplane forces; $\{q_z\}$ and $\{q_x\}$ are vectors with L elements. The matrix $[Q]$ results after approximating the derivative of M_b with finite differences. Its dimensions are also $L \times L$.

For the beam axial deformation problem, the solution of Eq. (10) is given in integral form as (Banerjee and Butterfield, 1981)

$$u_b(x) = -\int_0^l u_b^* q_x ds + \left[u_b^* \frac{du_b}{dx} - \frac{du_b^*}{dx} u_b \right]_0^l \tag{35}$$

where

$$u_b^* = \frac{1}{2E_b A_b} (l - |r|) \tag{36}$$

Following the same procedure as for the beam bending problem the axial force at the neutral axis of the beam for homogeneous boundary conditions (11) ($c_3 = 0$) can be expressed as follows

$$\{N_b\} = [F_b]\{q_x\} \tag{37}$$

where $[F_b]$ is known matrix with dimensions $L \times L$.

Eqs. (26) and (34) after elimination of the quantities N_x, N_y, N_{xy}, N_b using Eqs. (27a)–(27c) and (37) together with continuity conditions (12) and (13) which after discretization at the L nodal points at the interfaces are written as

$$\{w_p\} = \{w_b\} \tag{38a}$$

$$\{u_p\} - \frac{h_p}{2}\{w_{p,x}\} = \{u_b\} + \frac{h_b}{2}\{w_{b,x}\} \tag{38b}$$

constitute a nonlinear system of equations with respect to q_z, q_x, q_p, q_b. This system is solved using iterative numerical methods. Note that in Eqs. (38a) and (38b) the column matrices $\{u_p\}$, $\{u_b\}$ are evaluated from the relations

$$\{u_p\} = \lfloor F_p \rfloor\{q_x\} \tag{39a}$$

$$\{u_b\} = [F_b]\{q_x\} \tag{39b}$$

where $[F_p]$, $[F_b]$ are known $L \times L$ flexibility coefficient matrices the elements of which are evaluated numerically following the steps of the AEM.

Following the solution of the aforementioned system of equations the evaluation of the effective breadth is accomplished using any of the Eqs. (14), (15) or (16) after the calculation of the axial stresses σ_x using Eq. (20).

4. Numerical examples

On the basis of the analytical and numerical procedures presented in the previous sections, a computer program has been written and representative examples have been studied to demonstrate the efficiency and the range of applications of the developed method. In all the examples treated, the numerical results have been obtained using 54 constant boundary elements and 162 constant domain rectangular cells ($E = 3.0 \times 10^7$ kN/m^2, $h_p = 0.20$ m, $v = 0.154$).

Example 1: A rectangular plate with dimensions $a \times b = 18.0 \times 9.0$ m subjected to a uniform load $g = 10$ kN/m^2 and stiffened by a beam with width 1.0 m through the center line of the plate has been studied. The plate is simply supported along its small edges, while the other two edges are free. In Fig. 5 the contour lines of the total axial stresses σ_x for different heights of the stiffening beam are presented. It is worth noting that as the beam height increases the obtained values of the axial stresses are also increased due to the rise of the interface forces q_x.

After the evaluation of the axial stresses σ_x at the plate of the stiffened structure, the estimated values of the effective breadth according to Timoshenko and Goodier (1951) for different heights of the stiffening beam are presented in Fig. 6. From this figure it is easily concluded that the values of the effective breadth are not constant along the stiffening beam increasing from the supported edges to the center of the stiffened structure. Also, the variation of the effective breadth is significantly reduced as the beam height is increased.

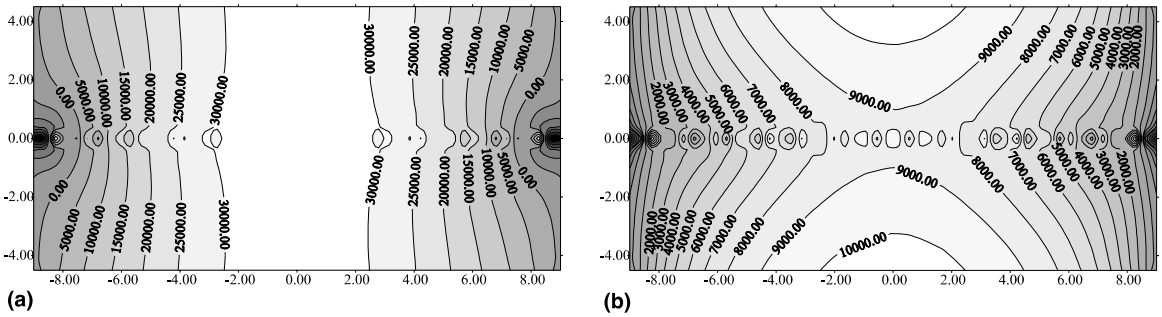

Fig. 5. Contour lines of the total axial stresses σ_x for (a) $h_b = 0.20$ m and (b) $h_b = 1.25$ m of the stiffened plate of Example 1.

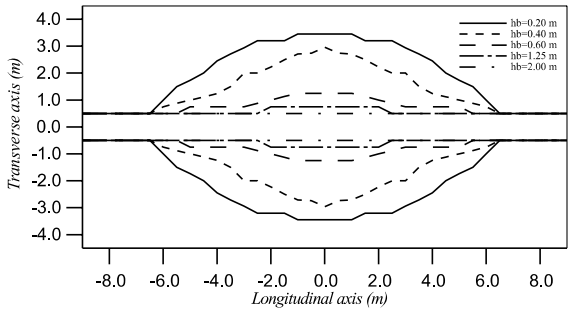

Fig. 6. Effective breadth according to the definition of Timoshenko and Goodier (1951) of the stiffened plate of Example 1 for various heights of the stiffening beam.

Moreover, in Fig. 7 the estimated values of the effective breadth according to Timoshenko and Goodier (1951) are presented as compared with those obtained according to all other available definitions (Schade, 1951; Wang and Rammerstorfer, 1996; Lee, 1962) for the beam height $h_b = 0.20$ m. From this figure it is easily concluded that the values of the effective breadth according to various definitions are almost identical.

Finally, in Figs. 8 and 9 the estimated values of the effective breadth for the beam heights $h_b = 0.20$ m and $h_b = 1.25$ m according to Timoshenko and Goodier (1951) are presented as compared with those

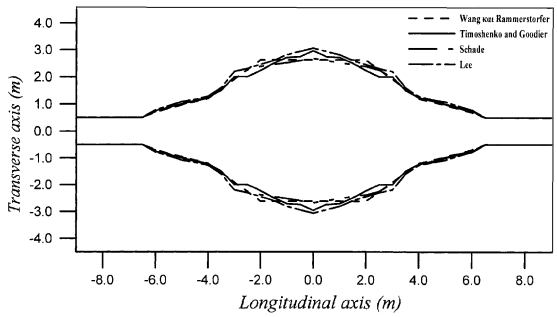

Fig. 7. Effective breadth according to the definitions of Timoshenko and Goodier (1951), Wang and Rammerstorfer (1996), Schade (1951) and Lee (1962) of the stiffened plate of Example 1 for $h_b = 0.40$ m.

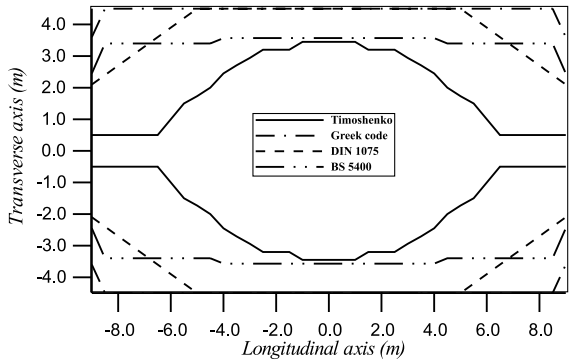

Fig. 8. Effective breadth of the stiffened plate of Example 1 for $h_b = 0.20$ m compared with the recommendations of various codes.

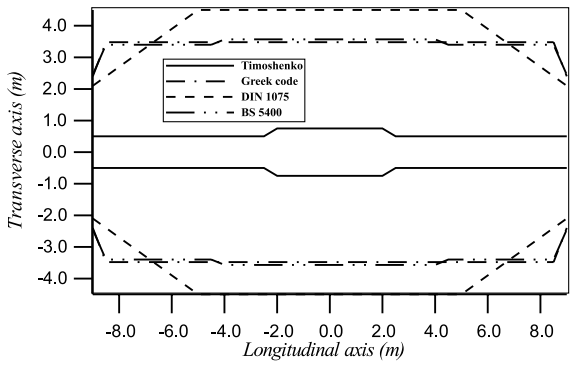

Fig. 9. Effective breadth of the stiffened plate of Example 1 for $h_b = 1.25$ m compared with the recommendations of various codes.

obtained from various codes. The discrepancy between the estimated values and the code proposed ones is remarkable.

Example 2: The stiffened plate of example 1 subjected to a uniform load $g = 10$ kN/m^2 for various heights of the stiffening beam has been studied and the values of the interface forces q_z, of the effective

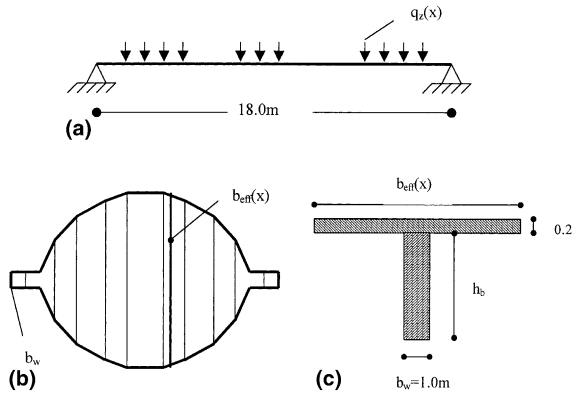

Fig. 10. Equivalent simply supported beam of variable cross-section subjected to the interface forces q_z (a), plan view (b) and transverse cross-section (c).

Table 1
Deflections $w(m)$ at $L/2$ (center) and $L/4$ of the beam of the stiffened plate of Example 2 (AEM) compared with those obtained from a 3-D FEM solution and from the equivalent beam for various beam heights

Beam	$L/2$ (Center)			$L/4$		
	AEM	FEM	Equivalent beam	AEM	FEM	Equivalent beam
1.0×2.00	3.4110E−04	3.910E−04	4.5900E−03	1.9960E−04	2.021E−04	3.2800E−03
1.0×1.25	1.1850E−03	1.228E−03	1.4990E−02	6.8720E−04	6.953E−04	1.0850E−02
1.0×0.60	7.6400E−03	7.860E−03	7.3800E−02	4.4070E−03	4.541E−03	5.4150E−02
1.0×0.40	1.9240E−02	1.995E−02	1.3432E−01	1.1150E−02	1.181E−02	9.9840E−02
1.0×0.20	6.6100E−02	6.782E−02	3.8264E−01	3.9470E−02	4.010E−02	2.8352E−01

breadth and of the deflections along the axis of the beam have been calculated. In Fig. 11 and in Table 1 these deflections (AEM) are presented as compared with those obtained from the solution of an equivalent simply supported beam subjected to the interface forces q_z and having variable cross-section consisting of the cross-section of the beam and a part of the plate corresponding to the estimated effective breadth (Fig. 10). The discrepancy of the obtained results necessitates the consideration of the inplane forces and deformations, which in the case of the simply supported beam have been neglected. Moreover, for justification of the accuracy of the results of the proposed model, in Table 1 the aforementioned obtained deflections (AEM) are compared with those obtained from an accepted finite element code (Sofistik, 1995) solving the corresponding three-dimensional elasticity problem (FEM). Very good agreement is easily verified.

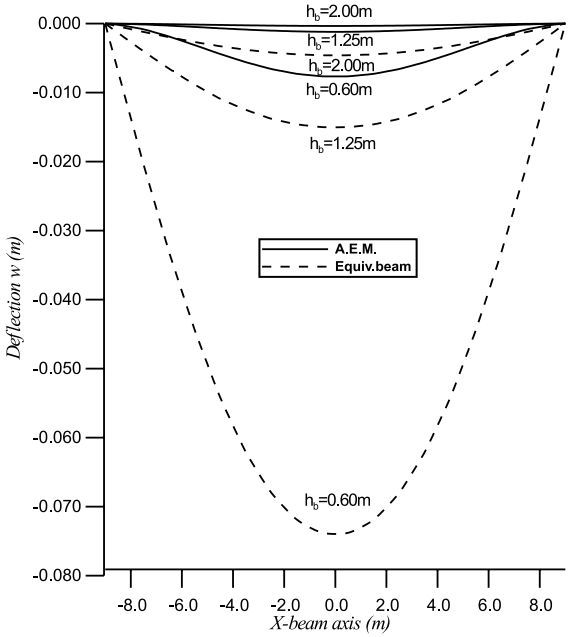

Fig. 11. Deflections $w(m)$ along the beam axis of the stiffened plate (AEM) compared with those of the equivalent beam of Example 2 for various beam heights.

5. Concluding remarks

In this paper a realistic estimation of the effective breadth of a stiffened plate has been presented. For the estimation of the effective breadth the adopted model contrary to the models used previously takes into account the resulting inplane forces and deformations of the plate as well as the axial forces and deformations of the beam. The main conclusions that can be drawn from this investigation are:

(a) The values of the effective breadth are not constant along the stiffening beam increasing from the supported edges to the center of the stiffened structure. Also, the variation of the effective breadth is significantly reduced as the beam height is increased.
(b) The values of the effective breadth according to various definitions given from various researchers are almost identical.
(c) The discrepancy between the estimated values of the effective breadth using the presented procedure and the code proposed ones is remarkable. It is worth here noting that most of the code proposed values are independent from the height of the stiffening beam.
(d) The discrepancy of the obtained deflections using the proposed model and an equivalent simply supported beam having variable cross-section according to the estimated effective breadth and subjected to the transverse interface forces necessitates the consideration of the inplane forces and deformations.

References

Banerjee, P.K., Butterfield, R., 1981. Boundary Element Methods in Engineering Science. McGraw-Hill, New York.
Katsikadelis, J.T., Kandilas, C.B., 1994. Solving the elastostatic problem by the analog equation method. Advances in Computational Mechanics, 178–269.
Lee, J.A.N., 1962. Effective Width of Tee-Beams. The Structural Engineer, January 21–27.
Sapountzakis, E.J., Katsikadelis, J.T., 2000. Analysis of plates reinforced with beams. Computational Mechanics 26, 66–74.
Schade, H.A., 1951. The effective breadth of stiffened plating under bending loads. Transactions of the Society of Naval Architects and Marine Engineers 59, 403–420.
Sofistik, GmbH. 1995. Software für Statik und Konstruktion Gesellschaft mit beschränkter Haftung, Ringstr. 29a, D-8042, Oberschleißheim.
Timoshenko, S.P., Goodier, J.H., 1951. In: Theory of Elasticity. McGraw-Hill, New York, pp. 262–268.
Tsutomu, U., 1982. Post-buckling of plates in compression and bending. Journal of the Structural Division, ASCE 108 (ST3), 591–609.
Tsutomu, U., 1993. Effective width of locally buckled plates in compression and bending. Journal of Structural Engineering, ASCE 119 (5), 1358–1373.
Wang, X., Rammerstorfer, F.G., 1996. Determination of effective breadth and effective width of stiffened plates by finite strip analysis. Thin-Walled Structures 26 (24), 261–286.